

Received: 29th March 2022

Revised: 28th April 2022

Accepted: 25th May 2022

BLOODSTAIN CLASSIFICATION IN HYPERSPECTRAL IMAGES USING A 3D DENSE CONVOLUTIONAL NEURAL NETWORK**TEJASKUMAR B. SHETH, HIMANSHUKUMAR D. NAYAK AND AVANIA A. VITHALANI****ABSTRACT:**

Bloodstains are often key evidence in forensic investigations, helping to piece together events at a crime scene and connect individuals to the incident. Traditional chemical methods used to detect blood, although effective, can damage the sample and interfere with further analyses like DNA profiling. In this study, we explore the use of deep learning models—specifically 2D CNNs, 3D CNNs, and Dense networks—for classifying bloodstains in hyperspectral images. We work with a publicly available dataset containing both real and synthetic blood samples, as well as substances commonly mistaken for blood, such as ketchup, beetroot juice, acrylic paint, and artificial blood. These samples are captured across 128 spectral bands in the 377–1046 nm range. We evaluate the performance of a custom-designed 2D CNN, 3D CNN, and a 3D Dense CNN network, all optimised for processing the high-dimensional nature of hyperspectral data. Our tests, done with different training and testing setups, show that the 3D Dense CNN provides better classification accuracy, clearer segmentation, and is more reliable in difficult situations. When compared with other leading CNN architectures, our proposed models consistently outperform, especially when training data is limited, with an overall accuracy of 94.36%. These results demonstrate the strong potential of combining hyperspectral imaging with advanced deep learning techniques for precise, non-destructive bloodstain classification paving the way for practical, real-time forensic applications at crime scenes.

Keywords: Deep Learning, Convolution Neural Network, 3D Dense CNN, Hyperspectral Image Classification, Forensic science, Bloodstain Detection.

1. INTRODUCTION

Bloodstain identification is essential to forensic investigations since it is frequently used as crucial evidence to reconstruct crime scenes and connect suspects to illegal activity. Blood traces have traditionally been found using chemical techniques, such as the luminol reaction or light-based enhancement methods [1]. Although these methods are useful for making traces more visible, they are frequently detrimental and open to arbitrary interpretation. Above all, they have the potential to damage biological samples, rendering them unfit for use in subsequent forensic procedures such as retesting or DNA profiling[2].

To address these limitations, researchers have explored a variety of non-contact, non-destructive spectroscopic methods. More accurate and thorough molecular information is provided by methods including Raman spectroscopy, Nuclear Magnetic Resonance (NMR), Infrared (IR) spectroscopy, and Electron Paramagnetic Resonance (EPR). These techniques, however, usually only use spectral data, ignoring a bloodstain's spatial properties, which are frequently essential for precise identification and analysis [3].

Hyperspectral Imaging (HSI) offers a powerful alternative for forensic analysis. By combining traditional imaging with spectroscopy, HSI captures detailed information about both the colour (spectral data) and the structure (spatial data) of a scene. The result is a three-dimensional image stack, with each layer representing a narrow slice of the light spectrum [4]. This ability to record hundreds of wavelengths makes HSI especially useful for detecting materials like blood, which has a unique light absorption pattern due to haemoglobin—particularly in the visible and near-infrared (NIR) ranges[5]. Unlike chemical methods, HSI is completely non-contact and non-destructive, helping preserve evidence for further investigation, such as DNA analysis[6].

In this study, we focus on the application of HSI combined with deep learning models—specifically, convolutional neural networks (CNNs)—for accurate bloodstain classification in a forensic context. We evaluate several network architectures, including 2D CNNs, 3D CNNs, and dense networks, to classify a publicly available dataset containing real and synthetic blood samples, as well as common lookalike substances like ketchup, beetroot juice, acrylic paint, and artificial

This paper is organized as follows: Section 2 reviews related work in the field of HSI. Section 3 describes the methodology, including details about the dataset and experimental setup. Section 4 presents and analyses the results. Finally, Section 5 concludes the paper with a summary of key findings and insights.

2. RELATED WORKS

Over the past two decades, HSI has advanced rapidly, driven by deep learning and affordable equipment, expanding from remote sensing to fields like agriculture, food safety, biotechnology, and forensic science[7]. Recent research in HSI classification—particularly in remote sensing and related fields—demonstrates that deep learning (DL) significantly enhances accuracy [8].

Early research in HSI classification primarily focused on analyzing the spectral signatures of individual pixels using pixel-wise methods such as support vector machines (SVM) and logistic regression (LR). Due to the high dimensionality of HSIs, techniques like principal component analysis (PCA) were employed to extract features and reduce dimensionality[9], which helped improve classification accuracy. Since HSI involves three-dimensional data, DL models have been effectively used to extract spectral, spatial, and combined spectral-spatial features. Unlike traditional kernel-based or dimensionality reduction techniques, DL approaches can automatically learn complex features and handle non-linear relationships. Among various DL models such as Convolutional Neural Networks (CNNs), Long Short-Term Memory networks (LSTMs), Multilayer Perceptrons (MLPs), and Deep Belief Networks (DBNs), CNNs have consistently delivered superior performance in HSI classification-tasks[10].

In[11], the paper presents a non-destructive method for bloodstain identification using HSI that can identify blood samples with aging up to 3 days. In the work stated PCA was used with SVM, KNN, AN, and RNN. In[12], author compares the performance of different deep learning architectures 1D CNN, 2D CNN, 3D CNN, RNN with baseline results of Support Vector Machine (SVM) to identify the bloodstain. The various deep learning methods show 74-94% accuracy with training and testing sample of 75-25%. In study [13], the authors explore the novel use of hyperspectral imaging (HSI) for detecting and aging beverage stains on paper towels in forensic investigations.

They employ a convolutional autoencoder for dimensionality reduction and a support vector machine (SVM) for efficient classification. The approach demonstrates a promising non-contact, non-destructive method for analyzing trace evidence, filling a gap in traditional forensic techniques. In [14], the authors introduce the Dense Convolutional Network (DenseNet) architecture, which establishes direct connections between each layer and every other layer in a feed-forward manner, resulting in $L(L+1)/2$ connections. This dense connectivity is implemented by concatenating the feature maps from all preceding layers as inputs to each subsequent layer, while each layer's own feature maps serve as inputs to all following layers. The authors highlight that this dense connectivity pattern enhances feature propagation, promotes feature reuse, and reduces the total number of parameters in the network.

Our research focusses on using a PCA as preprocessing, paired with a Dense CNN architecture known for its compactness and great learning capacity, to improve HSI classification performance. Overall, this strategy simplifies the network, uses fewer parameters, decreases training and testing durations, and delivers good classification accuracy even with minimal training data.

3. METHODOLOGY

We use a hardware environment comprised of the Google Colab cloud platform and GPUs to evaluate the performance of our various deep learning models implementation.

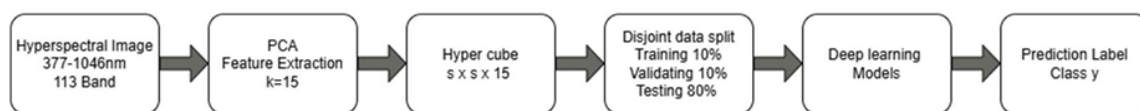


Figure 1. Overview of Implemented framework for HIS Classification

Figure 1. depicts the implemented framework for HSI classification. The HSI classification pipeline begins with a HSI acquired in the spectral range of 377–1046 nm comprising 113 bands. Next, Principal Component Analysis (PCA) is applied to reduce dimensionality, extracting the top 15 components ($k=15$). From the resulting data, an image hypercube of size $s \times s \times 15$ is generated. The dataset is then divided into disjoint subsets with 10% for training, 10% for validation, and 80% for testing. These subsets are fed into deep learning models for training and inference, culminating in the generation of prediction labels representing the identified class (y) of each pixel or patch.

Bloodstain detection dataset

Our experiments make use of HSI from the dataset described in [15], which is freely available to the public under an open license (the dataset can be assessed from <https://zenodo.org/record/3984905>). The dataset used in

this paper has HSIs of six different parts of one mock-up crime scene. The latter A-F are used to identify the different HSI frame as shown Figure 2. Images in datasets are acquired using a SOC710 hyperspectral camera in a spectral range of 377–1046 nm with a total of 128 bands. Images in the dataset were captured over several days to capture changes in spectra related to the time-related decay process of blood substances. Datasets images were annotated hyperspectral pixels accordingly the visible substance, so each HSI can be treated as labelled examples.



Figure 2. Illustration of the dataset, The mock-up of a forensic scene with locations of images A-F.

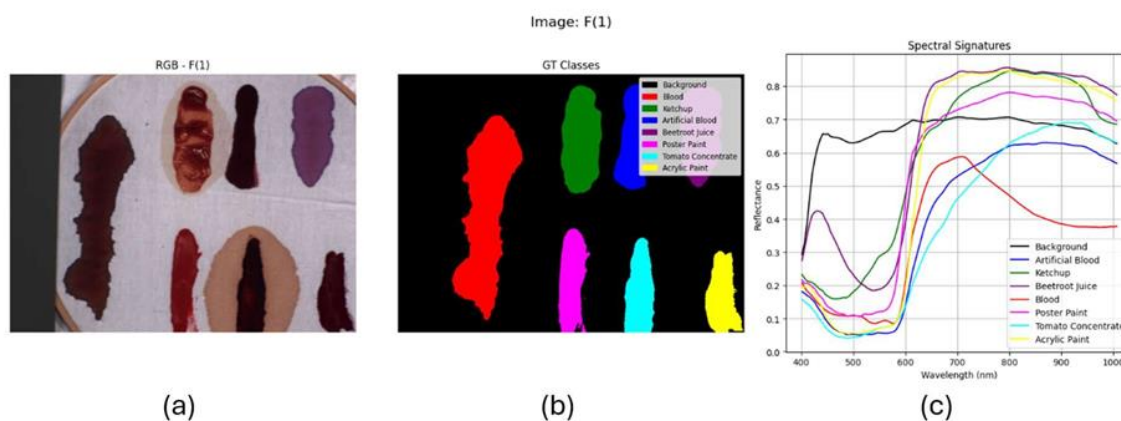


Figure 3. scene F 'Frame' (a) RGB Image of F(1) (b) Ground truth Image F(1) (c) Average spectral signature of substance present in image F(1)

Among the A to F scenes, the Scene F is specifically designed to capture detailed spectral data across multiple frames, each representing different conditions or variations of a bloodstain sample is used for our classification analysis. This setup mimics real-world forensic environments to ensure comprehensive data collection for developing robust bloodstain classification models. Frame F(1) captures the bloodstain in its original state, serving as a baseline for further analysis and comparison. Figure 3. illustrates the average spectral variation of blood across different frames in Scene F, highlighting significant changes due to time and varying illumination. The associated Table 1 displays the pixel-wise class annotations for this frame.

Table 1. Class wise annotated pixels distribution in image F(1)

Class	Substance Name	Number of Pixels
0	Background	267,361
1	Blood	29,598
2	Ketchup	14,177
3	Artificial Blood	9,603
4	Beetroot Juice	13,986
5	Poster Paint	9,290
6	Tomato Concentrate	8,938
7	Acrylic Paint	8,271

3D Dense CNN

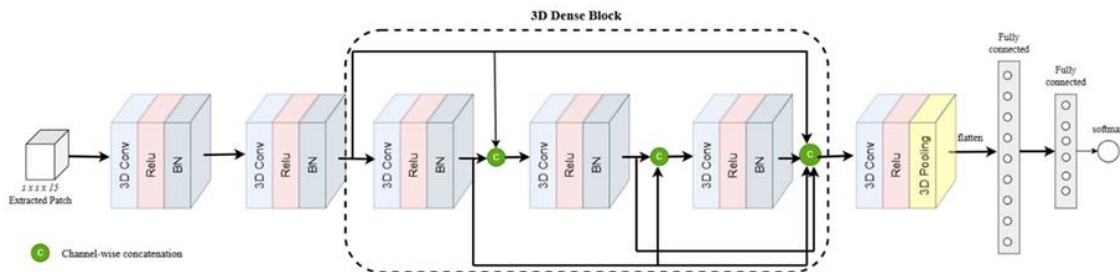


Figure 4. the proposed and implemented 3D dense CNN framework for HSI

The proposed 3D Dense Convolutional Neural Network (Dense CNN) model Figure 4. is designed to effectively classify HSI cubes by leveraging both spectral and spatial information. The architecture begins with three 3D convolutional layers that utilize 8 filters of size $3 \times 3 \times 3$ to extract fundamental spectral-spatial features from the input cube of size $9 \times 9 \times 15$. These are followed by three additional 3D convolutional layers, each with 16 filters of size $3 \times 3 \times 3$, which are densely connected to ensure feature reuse and gradient flow across layers. Dense connections allow concatenation of previous outputs to the input of subsequent layers, facilitating deeper network construction without the risk of vanishing gradients. Batch normalization follows each convolutional layer to improve training stability and reduce overfitting, and *ReLU* activations are applied to introduce non-linearity.

The final convolutional block includes a $1 \times 1 \times 1$ kernel to consolidate learned features, followed by a 3D pooling layer for spatial downsampling. The output is then flattened and passed through two fully connected layers (with 256 and 128 neurons, respectively), each followed by dropout regularization to prevent overfitting. The network concludes with a final dense layer that maps the features to the number of target classes (in this case, 7). The entire model is trained using the Adam optimizer and the *softmax* loss function for multi-class classification.

The proposed Dense CNN comprises approximately 75,703 trainable parameters and achieves a compact yet powerful design tailored for the classification of high-dimensional hyperspectral bloodstain data. The Table x Detailed structure of 3D Dense CNN model

Table 2. Detailed structure of Proposed 3D Dense CNN model

Layer	Output Shape	# Parameter
Input Layer	(9,9,15,1)	0
Conv3D_1 Batch Normalization_1	(7,7,9,8) (7,7,9,8)	512 32
Conv3D_2 Batch Normalization_2	(5,5,5,8) (5,5,5,8)	2888 32
Conv3D_3 Batch Normalization_3	(3,3,3,8) (3,3,3,8)	1736 32
Conv3D_4 Batch Normalization_4	(3,3,3,16) (3,3,3,16)	3472 64
Concatenation_1	(3,3,3,24)	0

Conv3D_5 Batch Normalization_5	(3,3,3,16) (3,3,3,16)	10384 64
Concatenation_2	(3,3,3,40)	0
Conv3D_6 Batch Normalization_6	(3,3,3,16) (3,3,3,16)	17296 64
Concatenation_3	(3,3,3,56)	0
Conv3D_7 Batch Normalization_7	(3,3,3,16) (3,3,3,16)	912 64
Flatten	16	0
Dense_1	256	4352
Dropout_1	256	0
Dense_2	128	32896
Dropout_2	128	0
Dense_3	7	903
Total Trainable Parameters		75,703

4. Experimental Result

To comprehensively evaluate the effectiveness of our deep learning architectures, we compared the performance of 2D CNN, 3D CNN, and 3D Dense CNN models using hyperspectral bloodstain data under three different cube window sizes: 9×9, 11×11, and 13×13. The experiments were conducted on Google Colab using GPU acceleration, with a fixed experimental configuration including an 80/10/10 train/validation/test split and a PCA reduction to 75 spectral components. The models were trained using the Adam optimizer (learning rate = 0.001) for ten epochs. The evaluation metrics include Overall Accuracy (OA), Average Accuracy (AA), and the Kappa Coefficient, and are presented in Table 3. Results clearly indicate that the 3D Dense CNN model consistently outperformed the other architectures across all window sizes. Notably, with a 9×9 cube size, the 3D Dense CNN achieved an OA of 94.36%, AA of 94.88%, and a Kappa value of 93.04%, surpassing both 2D and standard 3D CNNs.

In addition, a detailed classification report for the 3D Dense CNN model using the 9×9 configuration is shown in Table 4. The model demonstrated robust class-wise performance, with precision, recall, and F1-scores all above 0.90 for the majority of classes. Blood was classified with a high F1-score of 0.94, and confusing substances like ketchup and artificial blood were also distinguished effectively with F1-scores of 0.96 and 0.92, respectively. The macro and weighted averages of precision, recall, and F1-score all remained close to or above 0.94, validating the model's stability across all classes. These findings highlight the strength of our proposed 3D Dense CNN framework in hyperspectral bloodstain classification tasks, particularly in separating blood from other visually similar red-hued substances in forensic scenarios.

Table 3. Classification Accuracy Using 2DCNN,3DCNN, and 3D Dense, Performance

Method	Window Size	Overall Accuracy (OA)	Average Accuracy (AA)	Kappa Coefficient
2D CNN	9 × 9	83.27%	82.18%	81.41%
	11 × 11	82.91%	82.73%	81.89%
	13 × 13	81.21%	81.64%	81.45%
3D CNN	9 × 9	93.59%	91.77%	92.83%
	11 × 11	93.84%	92.29%	91.79%
	13 × 13	90.48%	86.55%	89.10%
3D Dense CNN	9 × 9	94.36%	94.88%	93.04%
	11 × 11	93.26%	92.30%	93.41%
	13 × 13	92.73%	90.25%	91.93%

Table 4. Classification Results using A 3D Dense CNN model with window size 9 x 9

Sample	Precision	Recall	F1-Score
Blood	0.96	0.92	0.94
Ketchup	0.95	0.97	0.96
Artificial Blood	0.91	0.93	0.92
Beetroot Juice	0.94	0.95	0.95
Poster Paint	0.97	0.96	0.96
Tomato Concentrate	0.92	0.90	0.91
Acrylic Paint	0.95	0.94	0.94
Accuracy	0.9436		

Macro avg	0.942	0.952	0.946
Weighted avg	0.944	0.948	0.945

5. CONCLUSION

In this study, the classification of bloodstains among various visually similar substances— including ketchup, artificial blood, beetroot juice, poster paint, tomato concentrate, and acrylic paint—was investigated using 2D CNN, 3D CNN, and 3D Dense CNN architectures. The HSIs data allowed the models to effectively distinguish between these red-hued substances, even in challenging mock crime scene conditions. Among the tested architectures, the 3D Dense CNN achieved the highest classification performance, with an overall accuracy of 94.36%, average accuracy of 94.88%, and a Kappa coefficient of 93.04% using a 9×9 spatial window and PCA-reduced bands.

These results highlight the strong potential of 3D Dense CNNs for real-time forensic applications, providing a non-invasive and chemical-free method to identify blood traces in complex scenarios. The dense connectivity and 3D spatial-spectral feature extraction in the model contributed significantly to its robust classification capabilities, even with limited training data. The class-wise metrics further validate its performance, with high precision and recall values across all categories.

The proposed approach confirms the viability of HSI combined with deep learning to automate blood detection, eliminating the dependence on expert interpretation or destructive analysis techniques. Future work may extend this research by incorporating transfer learning, testing the model on broader datasets, and applying it to real-world crime scene imagery for generalization and scalability assessment.

6. REFERENCES

- [1] V. Sharma and R. Kumar, “Trends of chemometrics in bloodstain investigations,” *TrAC Trends in Analytical Chemistry*, vol. 107, pp. 181–195, Oct. 2018, doi: 10.1016/j.trac.2018.08.006.
- [2] T. Sijen and S. Harbison, “On the Identification of Body Fluids and Tissues: A Crucial Link in the Investigation and Solution of Crime,” *Genes*, vol. 12, no. 11, p. 1728, Oct. 2021, doi: 10.3390/genes12111728.
- [3] S. Harbison and R. Fleming, “Forensic body fluid identification: state of the art,” *Research and Reports in Forensic Medical Science*, vol. 2016, no. 6, p. 11, Feb. 2016, doi: 10.2147/RRFMS.S57994.
- [4] N. Audebert, B. Saux, and S. Lefèvre, “Deep Learning for Classification of Hyperspectral Data: A Comparative Review,” *IEEE Geoscience and Remote Sensing Magazine*, vol. 7, no. 2, pp. 159–173, Apr. 2019, doi: 10.1109/MGRS.2019.2912563.
- [5] W. . Zijlstra and A. Buursma, “Spectrophotometry of Hemoglobin: Absorption Spectra of Bovine Oxyhemoglobin, Deoxyhemoglobin, Carboxyhemoglobin, and Methemoglobin,” *Comparative Biochemistry and Physiology Part B: Biochemistry and Molecular Biology*, vol. 118, no. 4, pp. 743–749, Dec. 1997, doi: 10.1016/S0305-0491(97)00230-7.
- [6] R. A. H. van Oorschot, K. N. Ballantyne, and R. J. Mitchell, “Forensic trace DNA: a review,” *Investigative Genetics*, vol. 1, no. 1, p. 14, Dec. 2010, doi: 10.1186/2041-2223-1-14.
- [7] R. Calvini, A. Ulrici, and J. M. Amigo, “Growing applications of hyperspectral and multispectral imaging,” in *Data Handling in Science and Technology*, vol. 32, 2019, pp. 605–629. doi: 10.1016/B978-0-444-63977-6.00024-9.
- [8] H. Data *et al.*, “Deep Learning-Based Classification of Deep Learning-Based Classification of Hyperspectral Data,” vol. 7, no. June 2014, pp. 1–14, 2015.
- [9] J. Su, D. Yi, C. Liu, L. Guo, and W.-H. Chen, “Dimension Reduction Aided Hyperspectral Image Classification with a Small-sized Training Dataset: Experimental Comparisons,” *Sensors*, vol. 17, no. 12, p. 2726, Nov. 2017, doi: 10.3390/s17122726.
- [10] M. E. Paoletti, J. M. Haut, J. Plaza, and A. Plaza, “Deep learning classifiers for hyperspectral imaging: A review,” *ISPRS Journal of Photogrammetry and Remote Sensing*, vol. 158, no. November 2018, pp. 279–317, 2019, doi: 10.1016/j.isprsjprs.2019.09.006.
- [11] M. Zulfiqar, M. Ahmad, A. Sohaib, M. Mazzara, and S. Distefano, “Hyperspectral Imaging for Bloodstain Identification,” *Sensors*, vol. 21, no. 9, p. 3045, Apr. 2021, doi: 10.3390/s21093045.

- [12] F. Pałka, W. Książek, P. Pławiak, M. Romaszewski, and K. Książek, “Hyperspectral classification of blood-like substances using machine learning methods combined with genetic algorithms in transductive and inductive scenarios,” *Sensors*, vol. 21, no. 7, Apr. 2021, doi: 10.3390/s21072293.
- [13] B. M. Devassy and S. George, “Forensic analysis of beverage stains using hyperspectral imaging,” *Scientific Reports*, vol. 11, pp. 1–13, 2021, doi: 10.1038/s41598-021-85737-x.
- [14] L. Zhi, X. Yu, B. Liu, and X. Wei, “A dense convolutional neural network for hyperspectral image classification,” *Remote Sensing Letters*, vol. 10, no. 1, pp. 59– 66, Jan. 2019, doi: 10.1080/2150704X.2018.1526424.
- [15] M. Romaszewski, P. Głomb, A. Sochan, and M. Cholewa, “A dataset for evaluating blood detection in hyperspectral images,” *Forensic science international*, vol. 320, p. 110701, Mar. 2021, doi: 10.1016/j.forsciint.2021.110701.

AUTHOR DETAILS

TEJASKUMAR B. SHETH¹, HIMANSHUKUMAR D. NAYAK² AND AVANIA. VITHALANI³

¹Associate Professor, Government Engineering College, Gandhinagar-28
tbsheth@gmail.com

²Assistance Professor, Government Engineering College, Gandhinagar-28
himanshu_mecse@yahoo.co.in

³Assistance Professor, Government Engineering College, Gandhinagar-28
avani@gecg28.ac.in